IMPLEMENTATION AND EVALUATION OF RANS TURBULENCE MODELS IN THE BRU3D CODE

Francisco José de Souza
Universidade Federal de Uberlândia
Uberlândia – MG – Brazil
e-mail: fjsouza@mecanica.ufu.br

Aristeu da Silveira Neto
Universidade Federal de Uberlândia
Uberlândia – MG – Brazil
e-mail: aristeus@mecanica.ufu.br

César José Deschamps
Universidade Federal de Santa Catarina
Florianópolis – SC – Brazil
e-mail: deschamps@nrva.ufsc.br

João Luiz F. Azevedo
Instituto de Aeronáutica e Espaço
CTA/IAE/ASE - N
e-mail: azevedo@iae.cta.br

Enda Dimitri Vieira Bigarella
Embraer – Empresa Brasileira de Aeronáutica
Av. Brigadeiro Faria Lima, 2170
12227-901 - São José dos Campos – SP – Brazil
e-mail: enda.bigarelli@embraer.com.br

Guilherme Lara de Oliveira
Embraer – Empresa Brasileira de Aeronáutica
São José dos Campos – SP – Brazil
e-mail: guilherme.oliveira@embraer.com.br

Abstract. *This paper describes the implementation and evaluation of two RANS turbulence models, namely the standard κ-ε model and the realizable κ-ε model in the Bru3D code. The baseline code is a 3D, unstructured, finite volume code originally developed at CTA/IAE. Along with the κ-ε models, two different wall treatments were evaluated: the standard logarithmic wall function and the enhanced wall treatment. In the latter, the two-layer κ-ε model is used along with the Kader wall function, which also holds for the viscous sublayer region. Results for different combinations of models and wall treatments were validated in two shear flows: compressible flow along flat plate and incompressible flow over backward facing step. The best results for the compressible flat plate flow were obtained with both κ-ε turbulence models combined with the enhanced wall treatment. For the backward facing step problem, the reverse flow as well as the redeveloping flow region were best predicted by the realizable κ-ε model integrated down to the wall, or combined with the enhanced wall treatment.*

Keywords*: RANS turbulence models, enhanced wall treatment, Bru3d.*

1. Introduction

Turbulence is one of the key phenomena in fluid dynamics. A major challenge in aerodynamic design is the accuracy of turbulence models for simulating complex turbulent flows. The choice of the appropriate turbulence model is then of paramount importance in a successful flow prediction. Development of improved turbulence models has increased in the last decade due to technological requirements. Nevertheless, the lack of information about their performance under different flow conditions has been a major obstacle for their effective use. Thus, validation and testing of turbulence models are still needed to understand their capabilities and limitations (Bardina et al, 1997).

In this paper, the implementation and evaluation of two Reynolds-averaged Navier-Stokes (RANS) turbulence models, namely the standard κ-ε model and the realizable κ-ε model, are considered. The models were implemented into the Bru3d code, which is an unstructured finite-volume based code developed at CTA/IAE (Scalabrin, 2002). Both models can be integrated up to wall but, nevertheless, two optional wall treatments are also provided: the standard logarithmic wall function and an enhanced wall treatment The latter combines the two-layer model in the near-wall region with the Kader wall function (Kader, 1981).

For the validation and evaluation of the implementations, two classical test cases for which experimental data are available have been chosen. The first test is the compressible flow over a flat plate, which allows one to check for implementations errors. The flow over a backward facing step is the second case and represents a challenge for most turbulence models, since separation, reattachment and redeveloping flow regions are present. The performance of different combinations of turbulence model and wall treatment were assessed with reference to experimental data for mean velocity profiles.

2. Formulation

2.1. Baseline code

The baseline code (Scalabrin, 2002) solves the compressible 3D Navier-Stokes equations in an unstructured, cell-centered, conservative finite-volume formulation. The equations are advanced in time with a five-step, second-order Runge-Kutta scheme. Diffusion transport terms are discretized with a second-order centered scheme whereas advection transport terms can be evaluated through either the Jameson scheme (Jameson et al, 1981 - centered with artificial dissipation) or the first-order Van Leer scheme. In all the simulations shown in this work, the Jameson scheme was used.

2.2. Standard κ-ε model

The κ-ε model is the most widely known and extensively used two-equation eddy viscosity model (Bardina et al, 1997). Different versions of this model are found in the literature. The formulation used here is the one of Launder and Sharma (1974), also referred to as the standard κ-ε model. The κ-ε model was originally developed to improve the mixing-length model and to avoid an algebraic prescription of the turbulence length scale in complex flows. This is made possible by solving transport equations for the turbulence kinetic energy, k, and for its dissipation rate, ε.

The eddy-viscosity in the standard κ-ε model is defined as a function of the turbulent kinetic energy, κ, and the turbulent dissipation rate, ε, as:

$$\mu_t = C_\mu f_\mu \rho \frac{\kappa^2}{\varepsilon} \tag{1}$$

The eddy viscosity is scaled with the fluid density, ρ, the turbulent velocity scale, $\kappa^{1/2}$, and the length-scale, $\kappa^{3/2}/\varepsilon$, based on local dimensional analysis. The model coefficient, C_μ, is determined by equilibrium analysis at high Reynolds numbers, and the damping function, f_μ, is modelled in terms of a turbulence Reynolds number, $\mathrm{Re}_t = \rho k^2/\varepsilon\mu$.

The standard κ-ε model equations for a compressible flow are:

$$\frac{\partial(\rho\kappa)}{\partial t} = P - \rho\varepsilon - \frac{\partial(\rho u_j \kappa)}{\partial x_j} + \frac{\partial}{\partial x_i}\left[\left(\mu_m + \frac{\mu_t}{\sigma_\kappa}\right)\frac{\partial \kappa}{\partial x_i}\right], \tag{2}$$

$$\frac{\partial(\rho\varepsilon)}{\partial t} = C_{\varepsilon 1}\frac{\varepsilon}{\kappa}P - f_2 C_{\varepsilon 2}\rho\frac{\varepsilon^2}{\kappa} - \frac{\partial(\rho u_j \varepsilon)}{\partial x_j} + \frac{\partial}{\partial x_i}\left[\left(\mu_m + \frac{\mu_t}{\sigma_\varepsilon}\right)\frac{\partial \varepsilon}{\partial x_i}\right], \tag{3}$$

where P is the production term, given by:

$$P = \mu_t\left[\left(\frac{\partial u_i}{\partial x_j} + \frac{\partial u_j}{\partial x_i}\right)\frac{\partial u_i}{\partial x_j} - \frac{2}{3}\left(\frac{\partial u_m}{\partial x_m}\right)^2\right] - \frac{2}{3}\rho\kappa\frac{\partial u_n}{\partial x_n}, \tag{4}$$

and f_2 is another near wall damping function.

The near wall damping functions f_μ and f_2 are expressed as:

$$\begin{aligned} f_\mu &= \exp\left[-3.4/(1+0.02\,\mathrm{Re}_t)^2\right] \\ f_2 &= 1 - 0.3\exp\left(-\mathrm{Re}_t^2\right) \end{aligned}. \tag{5}$$

Advection and diffusion transport terms were discretized with a first-order upwind and a second-order centered schemes, respectively. The equations for κ and ε are advanced in time with an implicit Euler scheme.

2.3. Realizable κ-ε model

The realizable k-ε model, proposed by Shih et al (1994), provides new formulations for the dissipation rate and eddy viscosity equations in order to improve the performance of the standard κ-ε model. The equation for the dissipation rate is based on the dynamic equation of the fluctuation vorticity. The new formulation for the eddy viscosity contains the effect of mean rotation on the turbulent stresses and ensures that normal stresses are always positive. Results for rotating homogeneous shear flows, free shear flows, channel flows, with and without pressure gradients, and flow over backward facing steps show that this model performs better than the standard κ-ε in almost all cases.

The eddy viscosity for this model is obtained from:

$$\mu_t = \min\left\{ C_\mu f_\mu \rho \frac{\kappa^2}{\varepsilon}, \frac{2\rho\kappa}{3S} \right\}, \tag{6}$$

where $S = \sqrt{2S_{ij}S_{ij}}$ is the magnitude of the rate of strain tensor S_{ij} and f_μ is a low-Reynolds number function, designed to account for viscous and inviscid damping turbulent fluctuations in the proximity of solid surfaces:

$$f_\mu = \frac{1-e^{-0.01\,\mathrm{Re}_t}}{1-e^{-\sqrt{\mathrm{Re}_t}}} \max\left\{1, \sqrt{\frac{2}{\mathrm{Re}_t}}\right\}. \tag{7}$$

The realizable κ-ε model consists of transport equation for κ, given by Eq. (2), and another for ε, which read:

$$\frac{\partial(\rho\varepsilon)}{\partial t} = \frac{(C_{\varepsilon 1}P - C_{\varepsilon 2}\rho\varepsilon + E)}{T_t} - \frac{\partial(\rho u_j \varepsilon)}{\partial x_j} + \frac{\partial}{\partial x_i}\left[\left(\mu_m + \frac{\mu_t}{\sigma_\varepsilon}\right)\frac{\partial\varepsilon}{\partial x_i}\right], \tag{8}$$

where P is the production term, given by Eq. (4). The additional term E in the dissipation-rate equation is designed to improve the model response to adverse pressure-gradient flows and is expressed as:

$$E = 0.3\rho\sqrt{\varepsilon T_t}\,\Psi \max\left\{\kappa^{1/2}, (\nu\varepsilon)^{1/4}\right\}, \tag{9}$$

$$\Psi = \max\left\{\frac{\partial\kappa}{\partial x_j}\frac{\partial(\kappa/\varepsilon)}{\partial x_j}\right\}. \tag{10}$$

The parameter T_t appearing in Eq. (8) is a realizable estimate of the turbulence timescale:

$$T_t = \frac{\kappa}{\varepsilon}\max\left\{1, \sqrt{\frac{2}{\mathrm{Re}_t}}\right\}. \tag{11}$$

As with the standard κ-ε model, for the advective and the diffusive terms, first-order upwind and second-order centered schemes were used, respectively. The discretization of transient terms is done by an implicit Euler scheme.

2.4. Logarithmic wall function

Most standard wall functions are based on the proposal of Launder and Spalding (1984):

$$u^+ = \frac{u_p}{u_\tau} = \frac{1}{\kappa}\ln y^+ + \frac{1}{\kappa}\ln E, \tag{12}$$

where u_p is the mean velocity parallel to the wall, u_τ is the friction velocity, $u_\tau = \sqrt{\tau_w/\rho}$, τ_w is the shear stress at the wall, E = 9.793, κ = 0.4187 is the von Karman constant and y^+ is the dimensionless distance from the wall:

$$y^+ = \frac{\rho u_\tau y}{\mu}. \tag{13}$$

It is often assumed that the flow is in local equilibrium, meaning that the production and dissipation are nearly equal. If this is the case, it can be shown that:

$$u_\tau = c_\mu^{1/4}\sqrt{k}\ . \tag{14}$$

It should be noted that the above boundary conditions are valid only when the first grid point is within the logarithmic region i.e. when $y^+>30$. In order to remedy this shortcoming of wall functions, the following operation is applied to Eq. (13):

$$\tilde{y}^+ = \max\left(y^+, 11.067\right), \tag{15}$$

that is, a lower limit is imposed on the value of y^+ (11.067), which marks the intersection between the logarithmic and the linear profile. As a consequence, the results are less dependent on the grid resolution, as shown in Vieser et al (2002).

2.5. Enhanced wall treatment

The enhanced wall treatment is a near-wall modeling method that combines a two-layer model with the Kader wall function. This enables a near-wall modeling that will possess the accuracy of the standard two-layer approach for refined near-wall meshes and that, at the same time, will not significantly reduce accuracy for coarser wall-function meshes. In the near-wall model implemented in the Bru3D code, the viscosity-affected near-wall region is completely resolved all the way through the viscous sublayer up to the wall. In this approach, the whole domain is subdivided into a viscosity-affected region and a fully-turbulent region. The demarcation of the two regions is determined by a wall-distance-based, turbulent Reynolds number, Re_y, defined as:

$$\mathrm{Re}_y = \frac{\rho y\sqrt{k}}{\mu}, \tag{16}$$

where y is the distance from the wall to the cell centers.
In the fully turbulent region ($\mathrm{Re}_y > \mathrm{Re}_y^*$, $\mathrm{Re}_y^*=200$), the standard k-ε model is employed. In the viscosity-affected near-wall region ($\mathrm{Re}_y < 200$), the one-equation model of Wolfstein is adopted. In the one-equation model, the momentum equations and the k equation are retained. However, the turbulent viscosity, μ_t, is computed from:

$$\mu_{t,2layer} = \rho C_\mu \ell_\mu \sqrt{k}\ , \tag{17}$$

where the length scale that appears in the equation above is computed from:

$$\ell_\mu = y c_\ell \left(1 - e^{-\mathrm{Re}_y/A_\mu}\right). \tag{18}$$

The two-layer formulation for turbulent viscosity described above is used as a part of the enhanced wall treatment, in which the two-layer definition is smoothly blended with the high-Reynolds-number μ_t definition from the outer region:

$$\mu_{t,enh} = \lambda_\varepsilon \mu_t + (1-\lambda_\varepsilon)\mu_{t,2layer}\ , \tag{19}$$

where μ_t is the high-Reynolds-number definition for the κ-ε model chosen, Eq.(1) or Eq.(6). A blending function, λ_ϵ, is defined in such a way that it is equal to unity far from walls and is zero very near walls. The blending function used is:

$$\lambda_\varepsilon = \frac{1}{2}\left[1 + \tanh\left(\frac{\mathrm{Re}_y - \mathrm{Re}_y^*}{A}\right)\right]. \tag{20}$$

The constant *A* in Eq. (20) determines the width of the blending function. By defining a width such that the value of $\lambda_\in$ will be within 1% of its far-field value given a variation of ΔRe_y, the result is:

$$A = \frac{\left|\Delta \mathrm{Re}_y\right|}{\tanh(0.98)}, \tag{21}$$

Typically, a value between 5% and 20% of Re_y* is assigned for ΔRe_y. The main purpose of the blending function $\lambda_\in$ is to guarantee solution convergence even when the κ-ε solution in the outer layer does not match well with the two-layer formulation.

The ε field is computed from:

$$\varepsilon = \frac{k^{3/2}}{\ell_\varepsilon}. \tag{22}$$

The length scale that appears in Eq. (22) is computed from Chen and Patel:

$$\ell_\varepsilon = y c_\ell \left(1 - e^{-\mathrm{Re}_y / A_\varepsilon}\right). \tag{23}$$

If the whole flow domain is inside the viscosity-affected region (Re_y < 200), ε is not obtained by solving its transport equation but instead from Eq. (22). The constants in the length scale formulas, Eqs. (18) and (23), are taken as:

$$c_\ell = \kappa c_\mu^{-3/4} \qquad A_\mu = 70 \qquad A_\varepsilon = 2c_\ell. \tag{24}$$

In order to have a method that can be applied throughout the near-wall region (i.e., viscous sublayer, buffer region, and fully-turbulent region) one has to formulate the law-of-the wall as a single fuction for the entire wall region. This can be achieved by blending linear and logarithmic laws-of-the-wall using a function suggested by Kader (1981):

$$u^+ = e^\Gamma u^+_{lam} + e^{1/\Gamma} u^+_{turb}, \tag{25}$$

where $y^+ = \dfrac{y}{\nu_\ell}\sqrt{\nu_\ell \dfrac{\partial u}{\partial y}}$ and $u^+ = u \Big/ \sqrt{\nu_\ell \dfrac{\partial u}{\partial y}}$

with the blending function given by:

$$\Gamma = -\frac{a\left(y^+\right)^4}{1 + b y^+}, \tag{26}$$

where $a = 0.01c$, $b = \dfrac{5}{c}$ and $c = 1.0$. (27)

Similarly, the general equation for the derivative $\dfrac{du^+}{dy^+}$ is:

$$\frac{du^+}{dy^+} = e^\Gamma \frac{du^+_{lam}}{dy^+} + e^{1/\Gamma} \frac{du^+_{turb}}{dy^+}. \tag{28}$$

This formula also guarantees the correct asymptotic behavior for large and small values of y^+ and reasonable representation of velocity profiles in the cases where y^+ falls inside the wall buffer region ($3 < y^+ < 10$).

3. Results and discussions

3.1. Compressible flat plate flow

In this test case, the numerical predictions were compared with the empirical correlations of mean velocity profile of a Mach 1.5 boundary layer flow over an adiabatic surface. The grid contains 10560 hexahedral elements, with special refinement near the wall. Further details on the setup of the simulation can be found in Scalabrin (2002). The Reynolds number was Re=10^6. There is a general consensus that the Van Driest I transformation (Van Driest, 1951) is a good fit to the experimental data of velocity profile in the inner layer:

$$u^+ = \frac{1}{0.41}\ln y^+ + 5 \tag{29}$$

Figure 1 presents the results of the standard and realizable κ-ε models integrated down to the wall and also combined with the logarithmic wall-function and the enhanced wall treatment. It can be seen that, when integrated down to the wall, the realizable κ-ε model provides a much better agreement with the experimental correlation. This is not a surprise since y+ for the first node away from the wall is nearly 0.6 and the standard κ-ε model requires this value to be around 0.1 to yield accurate results. The results of both turbulence models combined with the logarithmic wall function are seen to be very poor. Indeed, this mesh is fine enough to allow the first node away from the wall to lie in the linear region of the boundary-layer, where the logarithmic wall-function no longer holds. In fact, this wall function is only applicable when using a coarse mesh so that the first node from the wall lies in the logarithmic region. Both turbulence models combined with the enhanced wall treatment provide very similar profiles, which are in a considerably better agreement with the experimental data than the predictions.

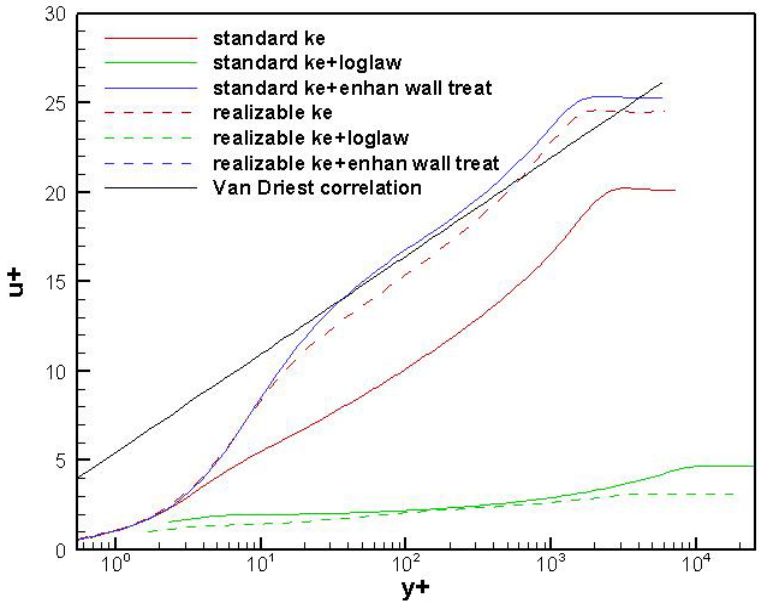

Figure 1. Vertical profiles of the dimensionless streamwise velocity for compressible flow along a flat plate (Re = 10^6, M_∞ = 1.5)

3.2. Backward facing step flow

The incompressible flow downstream of the step with an expansion ratio of 1.25 is modeled in this test case. The experiments were carried out by Vogel and Eaton (1984). The inlet is placed 3.8 H upstream of the step, whose height is H. The outlet boundary is located approximately 40 H downstream of the step. The Reynolds number, calculated as:

$$\mathrm{Re} = \frac{u_\infty H}{\nu_\infty}, \tag{30}$$

is 28,000 and the Mach number was kept at 0.3. All the walls were treated as adiabatic. In the experiment, the inlet profile evolved in a rectangular duct. Thus, the boundary layer profile at the inlet of the solution domain was imposed according to the experimental data (Vogel and Eaton, 1984). The mesh contains 14,190 hexahedral elements.

Figures 2(a) to 2(f) compare predictions and experimental data for mean streamwise velocity profiles at different stations downstream of the step. In the first station (Fig. 2a), the reverse flow is best predicted by the realizable κ-ε model with the enhanced wall treatment, while in the second station this model integrated to the wall provides the best

result, though overpredicting the mean profile above y/H=1. All the other combinations of turbulence models and wall functions underpredict the intensity of the recirculating flow region.

The redeveloping flow (Figs. 2c and 2d) close to the wall is best predicted by the realizable κ-ε model combined with the enhanced wall treatment, whereas all combinations associated to the standard κ-ε are shown to overpredict the velocity magnitude. However, the opposite trend is observed in the next stations (Figs. 2e and 2f), in which the standard κ-ε model combinations perform slightly better than any version of the realizable κ-ε. In this particular test case, it is important to bear in mind that the profiles also have the influence of the upper wall. Since experimental data above y/H=3 are not available, it is not possible to conclude that the numerical profiles display only the effect of the lower wall modeling, specially at stations away from the step where confinement effects are known to influence the results. Moreover, the value of y+ in the control volume next to the wall for most of the stations is above 1 in the mesh employed in these simulations.

4. Conclusions

This paper has presented the details of the implementation of two versions of k-ε turbulence models into the Bru3D code, which is a 3D, unstructured, finite volume code originally developed at CTA/IAE. The prediction capability of such models was analyzed with reference to a compressible boundary layer on a flat plate and an incompressible flow over backward facing step. Both models were tested for two wall treatments: the standard logarithmic wall function and the enhanced wall treatment. In the case of the boundary layer, the best results are achieved when both k-ε turbulence models are combined with the enhanced wall treatment. On the other hand, for the backward facing step problem, the best prediction was found with the realizable k-ε model. Overall, the results suggest that the best modeling strategy for the aforementioned flows is to combine the realizable k-ε model with the enhanced wall treatment.

5. Acknowledgements

The authors wish to thank Embraer for the support provided for this work.

The authors also acknowledge the support of Fundação de Amparo à Pesquisa do Estado de São Paulo, FAPESP, through the Research Grant No. 2000/13768-4.

6. References

Bardina, J. E., Huang, P. G. and Coakley, T. J., 1997, "Turbulence Modeling Validation, Testing and Development", NASA TM 110446.

Jameson, A., Schmidt, W. And Turkel, E., 1981, "Numerical Solution of the Euler Equations by Finite Volume Methods Using Runge-Kutta Time-Stepping Schemes", Proceedings of the AIAA 14th Fluid and Plasma Dynamics Conference, AIAA Paper no 81-1259, Palo Alto, CA.

Jones, W. P., and Launder, B. E., 1982, "The Prediction of Laminarization with a Two-Equation Model of Turbulence". International Journal of Heat and Mass Transfer, vol. 15, pp. 301-314.

Kader, B. A., 1981, "Temperature and Concentration Profiles in Fully Turbulent Boundary Layers". International Journal of Heat and Mass Transfer, vol. 24, pp. 1541-1544.

Kral, L. D., "Turbulence Modeling of Complex Flows", online report, www.nas.nasa.gov/Pubs/TechSums/9495/final6652.html.

Launder, B. E., and Sharma, B. I., 1974, "Application of the Energy Dissipation Model of Turbulence to the Calculation of Flow Near a Spinning Disc". Letters in Heat and Mass Transfer, vol. 1, no. 2, pp. 131-138.

Launder, B. E. and Spalding, D. B., 1984, "The Numerical Computation of Turbulent Flows", Comp. Meth. Appl. Mech. and Eng., vol. 3.

Scalabrin, L. C., 2002, Numerical Simulation of the Three-Dimensional Flows over Aerospace Configurations, Master's thesis, Instituto Tecnológico de Aeronáutica, São José dos Campos, SP, Brazil.

Shih, T. H., Liou, W. W., Shabbir, A. ,Yang, Z. and Zhu, J., 1994, "A New Eddy Viscosity Model for High Reynolds Number Turbulent Flows – Model Development and Validation". NASA TM 106721.

Van Driest, E. R., 1951, "Turbulent Boundary Layer in Compressible Fluids". J. Aeronaut. Sci., vol. 18, n. 3, pp.145-160.

Vieser, W., Esch, T. and Menter, F. R., 2002, "Heat Transfer Predictions using Advanced Two-Equation Turbulence Models", CFX Technical Memorandum CFX-VAL10/0602, pp.73.

Vogel, J. C. and Eaton, J. K., 1984, "Heat Transfer and Fluid Mechanics Measurements in the Turbulent Reattaching Flow Behind a Backward-Facing Step", Report MD-44, Thermosciences Division, Dept. of Mech. Engrg., Stanford University.

Wilcox, D. C., 1993, "Turbulence Modeling for CFD". DCW Industries, Inc, 5354 Palm Drive, La Cañada, Calif.

7. Responsibility notice

The authors are the only responsible for the printed material included in this paper.

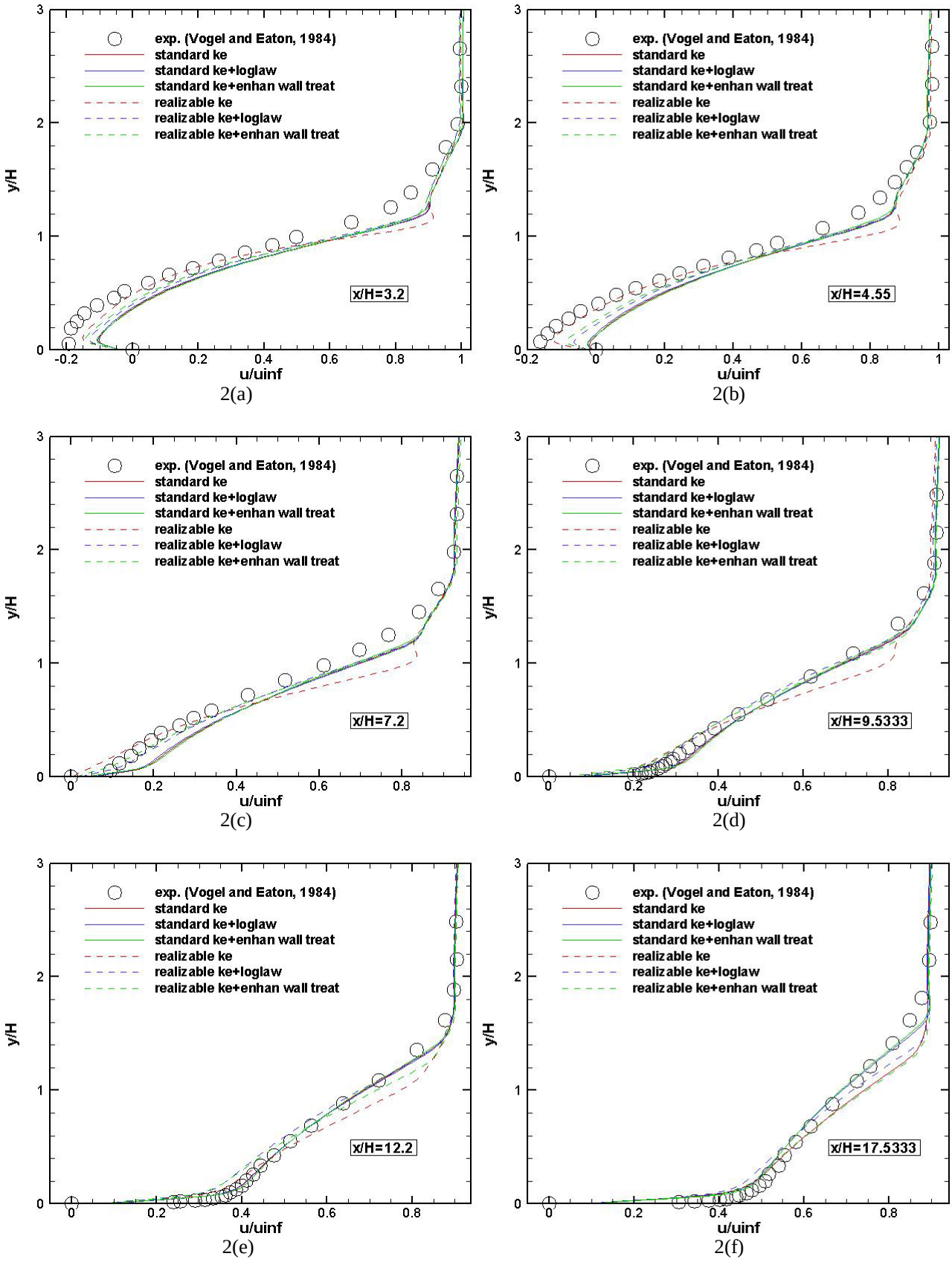

2(a) 2(b) 2(c) 2(d) 2(e) 2(f)

Figure 2. Vertical streamwise velocity profiles for the backward facing step flow: comparison between computed and experimental results at different horizontal stations downstream of the step.